Supersolid Bose-Fermi Mixtures in Optical Lattices

I. Titvinidze, M. Snoek, and W. Hofstetter

Institut für Theoretische Physik, Johann Wolfgang Goethe-Universität, 60438 Frankfurt am Main, Germany

We study a mixture of strongly interacting bosons and spinless fermions with on-site repulsion in a three-dimensional optical lattice. For this purpose we develop and apply a generalized dynamical mean-field theory, which is exact in infinite dimensions and reliably describes the full range from weak to strong coupling. We restrict ourselves to half filling. For weak Bose-Fermi repulsion a supersolid forms, in which bosonic superfluidity coexists with charge-density wave order. For stronger interspecies repulsion the bosons become localized while the charge-density wave order persists. The system is unstable against phase separation for weak repulsion among the bosons.

Ultracold atomic gases confined in optical lattices provide a new laboratory for investigating quantum many-body problems with high precision and tunability [1,2]. In this way new light can be shed on notoriously difficult problems in condensed matter physics [3]. One of the intriguing aspects of cold atoms is that the atomic quantum statistics can be controlled. In particular, cold atomic gases offer the possibility to realize mixtures of fermions and bosons [4–8], recently also in an optical lattice [9,10]. It is thus possible to create physical systems without analog in conventional solid state physics.

An exotic quantum phase that has intrigued researchers for a while is the *supersolid* with superfluid order, i.e., broken $U(1)$ symmetry, and coexisting particle density wave order. It is still an open question whether a supersolid has been realized in recent experiments on ^{4}He [11]. While in single-component quantum gases supersolids can only be stabilized by including nearest neighbor repulsion between the particles [12], they can be conveniently realized in Bose-Fermi mixtures with on-site repulsion as we show in this Letter. Earlier theoretical studies already suggested that Bose-Fermi mixtures can be unstable against charge-density wave (CDW) and supersolid order or phase separation (PS). However, so far all theoretical approaches either dealt with one-dimensional systems [13–19] or relied on weak-coupling approximations [20–22].

Here we introduce and apply a generalized dynamical mean-field theory (GDMFT) that treats this problem in a fully nonperturbative way. In this method the fermions are described by dynamical mean-field theory (DMFT) [23], into which the bosons are incorporated by means of the static Gutzwiller decoupling approximation [24] of the hopping. This approach therefore reproduces the strong coupling behavior of both the fermions and the bosons. In particular it is able to describe the formation of a bosonic Mott-insulator state for strong repulsion between the bosons at integer filling. Here we restrict ourselves to half filling for both the bosons and fermions ($\langle n_b \rangle = \langle n_f \rangle = \frac{1}{2}$). For weak interspecies repulsion we predict the formation of a *supersolid phase*, in which the bosons form a superfluid with spatially modulated density and the fermions

form a CDW. For stronger repulsion between the bosons and the fermions there is a first order phase transition to an *alternating Mott insulator* (AMI) plus CDW, in which the bosons become localized at every second lattice site while the fermionic charge-density wave persists. For weak bosonic repulsion we find an instability towards *phase separation*. We depict all these different phases schematically in Fig. 1.

A mixture of fermions and bosons in an optical lattice can be described by the single-band Fermi-Bose Hubbard model:

$$\mathcal{H} = -\sum_{\langle i,j \rangle} \{t_f c_i^\dagger c_j + t_b b_i^\dagger b_j\} - \sum_i \{\mu_f n_i^f + \mu_b n_i^b\}$$
$$+ \sum_i \left\{ \frac{U_b}{2} n_i^b (n_i^b - 1) + U_{fb} n_i^b n_i^f \right\}, \qquad (1)$$

where $c_i^\dagger$ $(b_i^\dagger)$ is the fermionic (bosonic) creation operator at site i, while $n_i^f = c_{i\sigma}^\dagger c_{i\sigma}$ $(n_i^b = b_i^\dagger b_i)$ denotes the num-
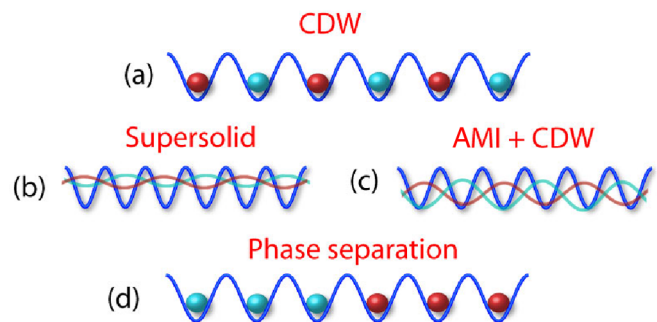

FIG. 1 (color online). Schematic structure of different $T = 0$ phases of a spinless Bose-Fermi mixture in an optical lattice. The dark (red) particles correspond to the fermions, while light (cyan) particles denote the bosons. In both the supersolid and the alternating Mott-insulator (AMI) phase the bosons and fermions have an alternating density pattern as depicted in (a). In the supersolid (b) the density oscillations are small and the bosons are superfluid. In the AMI + CDW phase (c) the density oscillations are large and the bosons are localized. The schematic structure of phase separation is depicted in (d).

ber operator and $\mu_{f(b)}$ the chemical potential for fermions (bosons). U_b and U_{fb} are the on-site boson-boson and fermion-boson interactions, respectively. $\langle i, j \rangle$ denotes summation over nearest neighbors, and $t_{f(b)}$ is the tunneling amplitude for fermions (bosons).

Following the very successful DMFT [23] and Gutzwiller [24] schemes, which are exact in infinite dimensions, we consider the infinite-dimensional limit ($d \to \infty$) of this model first, which is expected to be a good approximation to three spatial dimensions. In order to retain a finite kinetic energy the hopping parameters are rescaled as $t_f/\sqrt{d}$ and t_b/d. We then follow the standard "cavity derivation"; i.e., we consider a single impurity site and integrate out all other sites [23]. In the limit of infinite dimensions the only terms that survive in the effective action for the impurity site are the local terms, plus a bosonic source field and a fermionic (Weiss) mean field. The bosonic part corresponds to the Gutzwiller approximation, whereas the fermionic part corresponds to DMFT. Therefore, the GDMFT employed in our calculation consists of the DMFT algorithm for the fermions [23], combined with Gutzwiller mean-field theory for the bosons. Subsequently the action for the impurity site is mapped onto a generalized single impurity Anderson model (GSIAM). As usual, the impurity site is coupled to a noninteracting fermionic bath, which provides a self-consistent dynamical (Weiss) mean field [23]. In addition, the GSIAM now also contains a bosonic degree of freedom, which is self-consistently coupled to the superfluid order parameter, according to Gutzwiller mean-field theory [24]. In summary, the GSIAM is described by the following Hamiltonian, which allows for a two-sublattice structure:

$$\mathcal{H}_{\mathrm{GSIAM}} = \sum_{\sigma=\pm 1} [\mathcal{H}_b^\sigma + \mathcal{H}_{fb}^\sigma + \mathcal{H}_f^\sigma]$$

$$\mathcal{H}_b^\sigma = -zt_b(\varphi_{\bar{\sigma}} b_\sigma^\dagger + \varphi_{\bar{\sigma}}^* b_\sigma) + \frac{U_b}{2} n_\sigma^b(n_\sigma^b - 1) - \mu_b n_\sigma^b$$

$$\mathcal{H}_{fb}^\sigma = U_{fb} n_\sigma^f n_\sigma^b$$

$$\mathcal{H}_f^\sigma = -\mu_f n_\sigma^f + \sum_{\mathbf{k}} \{\varepsilon_{\mathbf{k}} a_{\mathbf{k}\sigma}^\dagger a_{\mathbf{k}\sigma} + V_{\mathbf{k}\sigma}(c_\sigma^\dagger a_{\mathbf{k}\sigma} + \mathrm{H.c.})\}.$$

$$(2)$$

Here σ is the sublattice index ($\bar{\sigma} = -\sigma$), z is the lattice coordination number, $\varphi_\sigma = \langle b_\sigma \rangle$ is the superfluid order parameter, and $V_{\mathbf{k}\sigma}$ are the fermionic hybridization matrix elements. The hybridization function is defined as $\Delta_\sigma(\omega) = \pi \sum_{\mathbf{k}} |V_{\mathbf{k}\sigma}|^2 \delta(\omega - \varepsilon_{\mathbf{k}})$. For convenience we perform our calculations on the Bethe lattice, which has a semielliptic noninteracting density of states $\rho(\varepsilon) = 2\sqrt{D^2 - \varepsilon^2}/\pi D^2$. Here $D = 2\sqrt{z}t_f$ is the noninteracting fermionic half-bandwidth. In the following we take D as the unit of energy. The fermionic DMFT self-consistency relation on the Bethe lattice has the form $\Delta_\sigma(\omega) = \frac{\pi}{4} A_{\bar{\sigma}}(\omega)$ [23], where $A_\sigma(\omega)$ is the local fermionic interact-

ing (impurity) spectral function. To calculate $A_\sigma(\omega)$ and $\varphi_\sigma = \langle b_\sigma \rangle$ from the GSIAM (2) we use the nonperturbative numerical renormalization group (NRG) technique [25,26]. The resulting hybridization function as obtained via the spectral function $A_\sigma(\omega)$ and the bosonic order parameter φ_σ determines the new coefficients of the GSIAM. This procedure is iterated until convergence is reached. The GDMFT approach incorporates the local correlations between bosons and fermions in a fully nonperturbative fashion and thus reliably describes the full range from weak to strong coupling. In our calculations we use a cutoff for the number of bosons on the impurity site, which can be kept low due to the repulsive interactions, which suppress multiple occupancy of the bosons. All of the results presented here are obtained at $T = 0$.

The self-consistent GDMFT procedure as described above can yield multiple stable solutions. To find the ground state of the system, we need to compare the energy of these solutions, which is given by

$$\frac{E}{N} = \frac{1}{N}\mathcal{H}_K + \frac{1}{2}\sum_{\sigma=\pm 1}\left(U_{fb}\langle n_\sigma^f n_\sigma^b \rangle + \frac{U_b}{2}\langle n_\sigma^b(n_\sigma^b - 1)\rangle\right),$$

$$(3)$$

where $\mathcal{H}_K/N = \frac{1}{2}\sum_\sigma \langle \mathcal{H}_f^\sigma \rangle - zt_b\varphi_{-1}\varphi_1$ and the indices ± 1 correspond to the two different sublattices. To calculate the fermionic part of the kinetic energy we use the same approach as for an antiferromagnetic state, which also has a two-sublattice structure [23,27]:

$$\frac{1}{N}\mathcal{H}_K = -zt_b\varphi_{-1}\varphi_1 + \int_{-\infty}^{\infty} d\varepsilon\varepsilon\rho(\varepsilon)\int_{-\infty}^{0} d\omega A(\varepsilon, \omega),$$

$$(4)$$

where $\rho(\varepsilon)$ is the fermionic noninteracting density of states
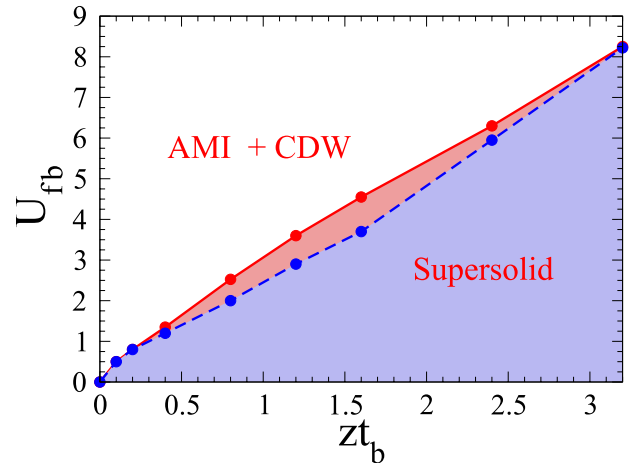

FIG. 2 (color online).   Phase diagram of the Fermi-Bose Hubbard model with spinless fermions and hard-core bosons at half filling. We identify the supersolid phase (below solid red line), the AMI phase with charge-density wave (CDW) (above solid red line), and the coexistence region (between the solid red line and dashed blue line). Energies are expressed in units of the noninteracting fermionic half-bandwidth D.

and $A(\varepsilon, \omega) = -\frac{1}{\pi} \operatorname{Im} \frac{1}{\sqrt{\zeta_{-1}\zeta_1} - \varepsilon}$ is the spectral function, with $\zeta_\sigma = \omega + \mu_f - \Sigma_\sigma(\omega)$ ($\sigma = \pm 1$). We calculate the self-energy following [28] $\Sigma(\omega) = U_{fb}F(\omega)/G(\omega)$ where $G(\omega)$ is the fermionic Green's function and $F(\omega) = \langle fb^\dagger bf^\dagger \rangle_\omega$.

We now first apply our GDMFT procedure to the limit $U_b = \infty$, i.e., hard-core bosons. We fix the number of bosons and fermions at half filling ($\langle n_b \rangle = \langle n_f \rangle = \frac{1}{2}$), which makes the system particle-hole symmetric. Without loss of generality, calculations are performed for repulsive Fermi-Bose interactions: $U_{fb} > 0$. The case of attractive interactions will be inferred later on with the help of a (staggered) particle-hole transformation. Since we take the noninteracting fermionic half-bandwidth D as the unit of energy, the bosonic hopping amplitude t_b and the interaction U_{fb} are the remaining adjustable parameters.

Our results are shown in the $U_{fb} - t_b$ phase diagram in Fig. 2. For weak repulsion between fermions and bosons we obtain a *supersolid phase* with a small CDW amplitude (see Fig. 3). For strong interactions between fermions and bosons we obtain a bosonic AMI together with a CDW of the fermions. In this phase the fermionic CDW amplitude $|\Delta N_f|$ is almost maximal, while the bosons are completely localized and have a CDW amplitude equal to $|\Delta N_b| = 0.5$. Taking into account virtual bosonic particle-hole excitations beyond Gutzwiller would however lead to a slightly smaller bosonic CDW amplitude. This transition is very similar to the one for bosons in a superlattice: upon increasing the potential difference between the sublattices there is a Mott-insulator transition at half filling [29]. For intermediate coupling both solutions are stable within GDMFT. To determine which of them corresponds to the ground state, we have compared their energies as given by

Eq. (3). We find that the supersolid phase always has the lower energy; i.e., the ground state is the supersolid. The coexistence of GDMFT solutions is a strong indication for a first order phase transition (at $T = 0$). As shown in Fig. 2, the critical value U_{fb}^c for the phase transition from the supersolid into the AMI phase increases with the bosonic tunneling amplitude.

The fermionic spectrum is always gapped. Spectral densities are shown in Fig. 4. The gap is small for the supersolid phase, but at the transition point there is a jump in the gap and in the AMI phase it becomes of the order of the noninteracting half-bandwidth D (see inset of Fig. 4). This implies that the latter phase will be more stable against finite temperature effects.

So far we have considered repulsive interactions between bosons and fermions. To see what happens for attractive interactions $U_{fb} < 0$ we apply a staggered particle-hole transformation to the fermions, $c_i \rightarrow (-1)^i c_i^\dagger$, which leads to a minus sign in front of the Bose-Fermi interaction term. This implies that for attractive interactions we obtain the same quantum phases, but the CDW oscillations are now in phase instead of out of phase as for repulsive interactions.

We now proceed by considering finite interactions between the bosons, i.e., relaxing the hard-core condition, but still assume the fermions and the boson to be half filled. We consider the case that the bosons are slightly slower than the fermions: $zt_b = 0.4D$. Our findings are summarized in the U_{fb}–U_b phase diagram in Fig. 5. For strong bosonic repulsion U_b the results are similar to the ones found for hard-core bosons: we find a supersolid for weak U_{fb} and the alternating Mott-insulator phase for stronger U_{fb}, separated by a first order transition. The critical interspecies repulsion at the transition between supersolid and the AMI phase increases when the value of the bosonic repulsion U_b
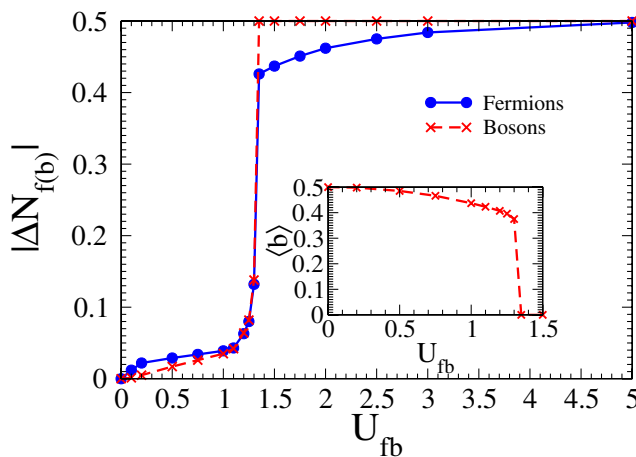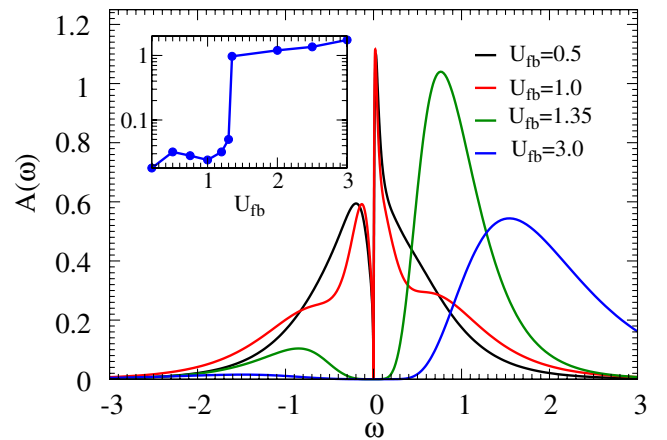

FIG. 3 (color online). Amplitude of the CDW for fermions (blue circles, solid line) and hard-core bosons (red crosses, dashed line) as a function of the fermion-boson interaction U_{fb} for the case when $zt_b = 0.4D$. In the inset we plot the bosonic superfluid order parameter as a function of the fermion-boson interaction U_{fb}.

FIG. 4 (color online). Fermionic spectral function in a mixture with hard-core bosons and $zt_b = 0.4D$ for different values of U_{fb}. In the inset we plot the size of the gap in units of D as a function of U_{fb}. The gap is defined by the frequencies for which the spectral function has half its maximal value.
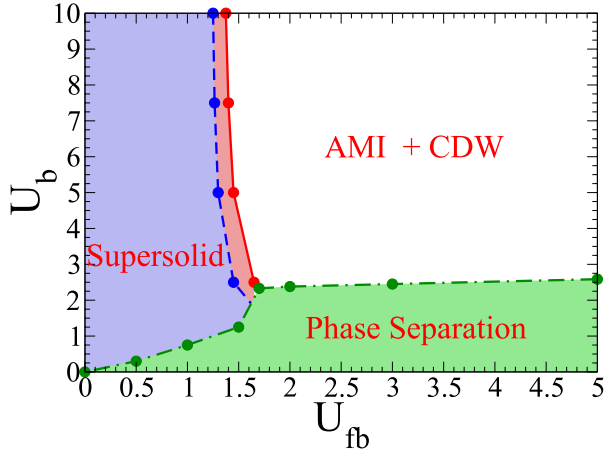
FIG. 5 (color online). Phase diagram of the Fermi-Bose Hubbard model with spinless fermions. Both fermions and bosons are half filled and $zt_b = 0.4D$. Stable phases are the supersolid (left of the solid red line and above the dash-dotted green line) and the AMI phase with CDW (right of the solid red line and above the dash-dotted green line). In the area between the solid red line and the dashed blue line both solutions are stable. Below the dash-dotted green line phase separation (PS) takes place.

is reduced. This is because the supersolid state acquires a lower energy when U_b is decreased, whereas the energy of the AMI phase remains the same. For weak interactions U_b among the bosons, the half filled state is unstable towards PS. In this parameter regime we do not find a converged GDMFT solution where the bosons and the fermions are half filled. To establish the occurrence of phase separation we also performed calculations away from half filling. We found a pronounced jump in the density as a function of the chemical potential and coexisting solutions close to the position of the jump. Moreover, we observed that for strong interspecies repulsion the phase separation is always complete. This allowed us to compare the energies of the PS and AMI states, which yields the dash-dotted (green) line as depicted in Fig. 5. We have checked that comparison of energies yields the same boundary for phase separation as deduced from the disappearance of a converged homogeneous GDMFT solution.

Also in this case we can infer the effect of attractive Bose-Fermi interactions by performing a staggered particle-hole transformation for the fermions. Phase separation turns then into phase separation of bosons and fermionic holes, which is equivalent to clustering of the bosonic and fermionic particles. So for weak repulsion U_b among the bosons a system with attractive interspecies interaction U_{fb} will maximize its density in part of the system, leaving the rest unoccupied.

In conclusion, we have studied a mixture of half filled spinless fermions and bosons in a three-dimensional optical lattice at zero temperature. We established the presence of a supersolid at weak Bose-Fermi repulsion. For strong

interspecies interaction a first order phase transition occurs towards a state where the bosons are localized and form an alternating Mott insulator. An instability towards phase separation was observed for weak interaction among the bosons.

[1] D. Jaksch *et al.*, Phys. Rev. Lett. **81**, 3108 (1998).
[2] M. Greiner *et al.*, Nature (London) **415**, 39 (2002).
[3] W. Hofstetter *et al.*, Phys. Rev. Lett. **89**, 220407 (2002).
[4] A. G. Truscott *et al.*, Science **291**, 2570 (2001).
[5] Z. Hadzibabic *et al.*, Phys. Rev. Lett. **91**, 160401 (2003).
[6] G. Roati *et al.*, Phys. Rev. Lett. **89**, 150403 (2002).
[7] C. Silber *et al.*, Phys. Rev. Lett. **95**, 170408 (2005).
[8] M. Zaccanti *et al.*, Phys. Rev. A **74**, 041605 (2006).
[9] S. Ospelkaus *et al.*, Phys. Rev. Lett. **96**, 180403 (2006).
[10] K. Günter *et al.*, Phys. Rev. Lett. **96**, 180402 (2006).
[11] E. Kim and M. Chan, Nature (London) **427**, 225 (2004); A. Leggett, Science **305**, 1921 (2004); N. Prokof'ev and B. Svistunov, Phys. Rev. Lett. **94**, 155302 (2005).
[12] P. Sengupta *et al.*, Phys. Rev. Lett. **94**, 207202 (2005); D. L. Kovrizhin *et al.*, Europhys. Lett. **72**, 162 (2005); V. W. Scarola and S. Das Sarma, Phys. Rev. Lett. **95**, 033003 (2005); S. Wessel and M. Troyer, Phys. Rev. Lett. **95**, 127205 (2005); D. Heidarian and K. Damle, Phys. Rev. Lett. **95**, 127206 (2005); R. G. Melko *et al.*, Phys. Rev. Lett. **95**, 127207 (2005); G. G. Batrouni *et al.*, Phys. Rev. Lett. **97**, 087209 (2006).
[13] L. Mathey *et al.*, Phys. Rev. Lett. **97**, 030601 (2006).
[14] L. Pollet *et al.*, Phys. Rev. Lett. **96**, 190402 (2006).
[15] A. Imambekov and E. Demler, Phys. Rev. A **73**, 021602(R) (2006).
[16] L. Mathey *et al.*, Phys. Rev. Lett. **93**, 120404 (2004).
[17] R. Roth and K. Burnett, Phys. Rev. A **69**, 021601 (2004).
[18] M. A. Cazalilla and A. F. Ho, Phys. Rev. Lett. **91**, 150403 (2003).
[19] A. Albus *et al.*, Phys. Rev. A **68**, 023606 (2003).
[20] H. P. Büchler and G. Blatter, Phys. Rev. Lett. **91**, 130404 (2003).
[21] M. Lewenstein *et al.*, Phys. Rev. Lett. **92**, 050401 (2004).
[22] F. D. Klironomos and S.-W. Tsai, Phys. Rev. Lett. **99**, 100401 (2007).
[23] W. Metzner and D. Vollhardt, Phys. Rev. Lett. **62**, 324 (1989); A. Georges *et al.*, Rev. Mod. Phys. **68**, 13 (1996).
[24] D. S. Rokhsar and B. G. Kotliar, Phys. Rev. B **44**, 10 328 (1991); K. Sheshadri *et al.*, Europhys. Lett. **22**, 257 (1993).
[25] G. Wilson, Rev. Mod. Phys. **47**, 773 (1975); W. Hofstetter, Phys. Rev. Lett. **85**, 1508 (2000).
[26] We use the NRG parameters $\Lambda = 2.0$, $N_{iter} = 60$, and $N = 1000$ kept states (using N_f as a good quantum number). The bosonic number cutoff is set to 4.
[27] R. Zitzler *et al.*, Eur. Phys. J. B **27**, 473 (2002).
[28] R. Bulla *et al.*, J. Phys. Condens. Matter **10**, 8365 (1998).
[29] V. G. Rousseau *et al.*, Phys. Rev. B **73**, 174516 (2006).